Circuit and Electromagnetic System Design Notes

Note 59

4 February 2009

Variations on the Switched-Oscillator Theme

Carl E. Baum
University of New Mexico
Department of Electrical and Computer Engineering
Albuquerque New Mexico 87131

Abstract

This paper extends the design options for switched oscillators. The oscillator length is increased for a given frequency, up to a full wavelength for the differential version. Multiax cable topology is fundamental to these extensions.

`

This work was sponsored in part by the Air Force Office of Scientific Research.

1. Introduction

The switched oscillator is proving to be a useful source for producing mesoband high-power waveforms [2-4, 8, 10, 11]. Beginning with the basic single-ended concept [8], the concept has extended to differential designs [3, 4]. By use with transmission-line transformers [9] one can go to higher-characteristic-impedance oscillators [10] which allow for greater available energy for a given oscillator frequency.

Here we consider some additional techniques for extending the performance of switched oscillators. The initial concept involves a quarter-wave transmission-line oscillator triggered at the opposite end from a relatively high-impedance load (antenna) [4]. By making this differential we obtained a half-wave transmission-line oscillator, switched in the center, driving two high-impedance loads at opposite ends.

Recollecting some techniques used for special electromagnetic sensors, perhaps they can be applied to our current problem. Specifically, one might use a multiax coaxial geometry in which signals propagate in a nested way with transmission lines inside transmission lines [1]. This may allow us to increase the electrical length of our transmission lines, and, hence, physical length for a given frequency.

2. Full-Wavelength Differential Oscillator

As a first-step consider the configuration in Fig. 2.1. by having a low impedance (large admittance $s\mathrm{C}_t$) at both ends of a transmission line we can have a resonance where the line length is a full wavelength, λ_1. The voltage is minimal at both ends and is zero in the middle to coincide with the basic symmetry of the charging potential (antisymmetric [12]). The current is maximum at both ends and in the center. Later considerations will concern how to reduce C_t.

The next question concerns how to extract the signal from this full-wave oscillator. We might think of sampling the current at ends or center, or the voltage at quarter-wave positions away from the switch. We also need to make the coupling sufficiently small so as not to greatly perturb the basic resonant mode.

As shown in Fig. 2.2, we have an equivalent transmission-line circuit. Each half has length ℓ_0 with

$$\begin{aligned} T_0 &= 2\frac{\ell_0}{\mathrm{v}} \equiv \text{period of oscillation} \\ &= f_1^{-1} \\ \mathrm{v} &\simeq \mathrm{c} \text{ (speed of light) for gas dielectric} \\ Z_c &\equiv \text{transmission-line characteristic impedance} \end{aligned} \tag{2.1}$$

This applies to the change after switch closure (neglecting the initial DC charge voltage). Let us approximate the loads as short circuits with

$$\mathrm{C}_t \simeq \infty \tag{2.2}$$

Then we have ideal waveforms as in Fig. 2.3. The current behaves as a staircase with all changes in the same direction. The voltage, however, behaves as a square wave superimposed on a DC shift of $V_0/2$. It is these waveforms that we need to sample and drive some radiating load (antenna) at frequency f_1.

For our analysis we have

$$\begin{aligned} s &= \Omega + j\omega \equiv \text{Laplace-transform variable or complex frequency} \\ \sim &\equiv \text{two-sided Laplace transform} \\ s_1 &= j\omega_1 \equiv \text{ideal complex resonant frequency} \\ \omega_1 &= 2\pi f_1 \equiv \text{ideal resonant frequency} \\ \gamma &\equiv \frac{s}{\mathrm{v}} \equiv \text{propagation constant in oscillator} \\ \lambda_1 &= \frac{\mathrm{v}}{f_1} \equiv \text{ideal resonant wavelength} \end{aligned} \tag{2.3}$$

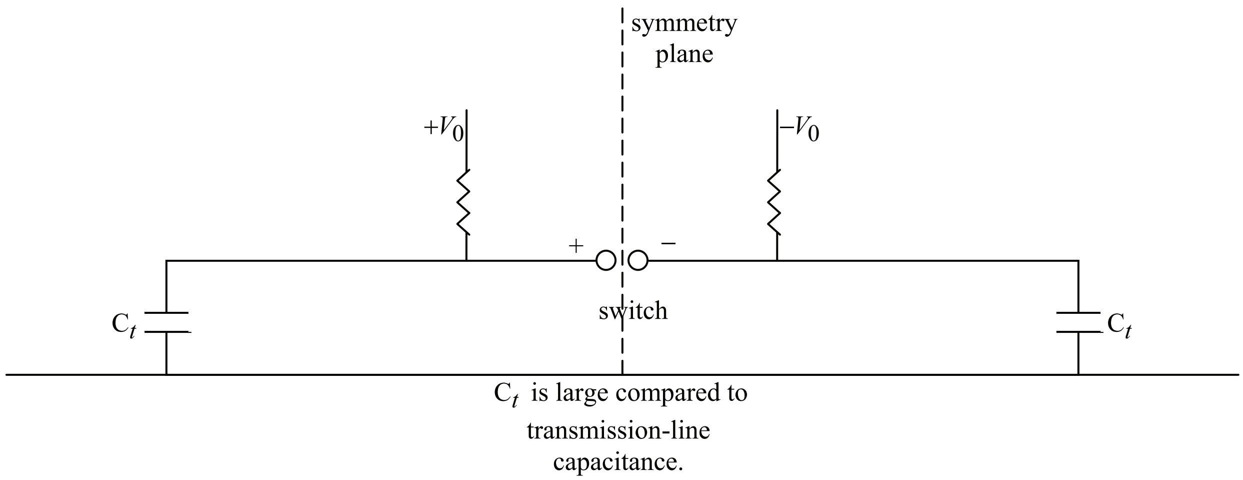

A. Before switch closure

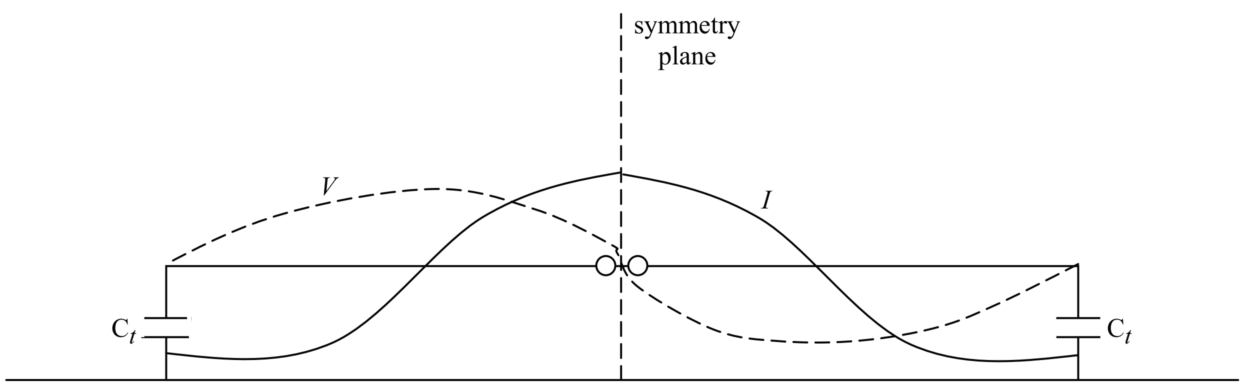

B. After switch closure: asic antisymmetric mode

Fig. 2.1 Full-Wavelength Oscillator

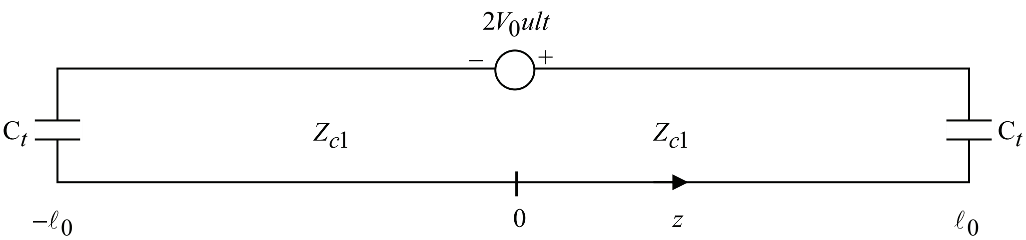

Fig. 2.2 Ideal Equivalent Circuit

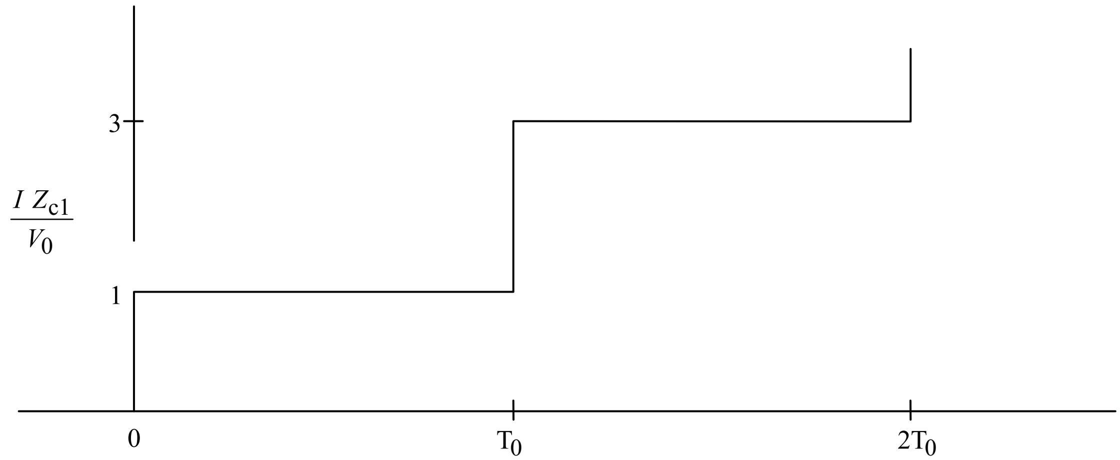

A. Current at source

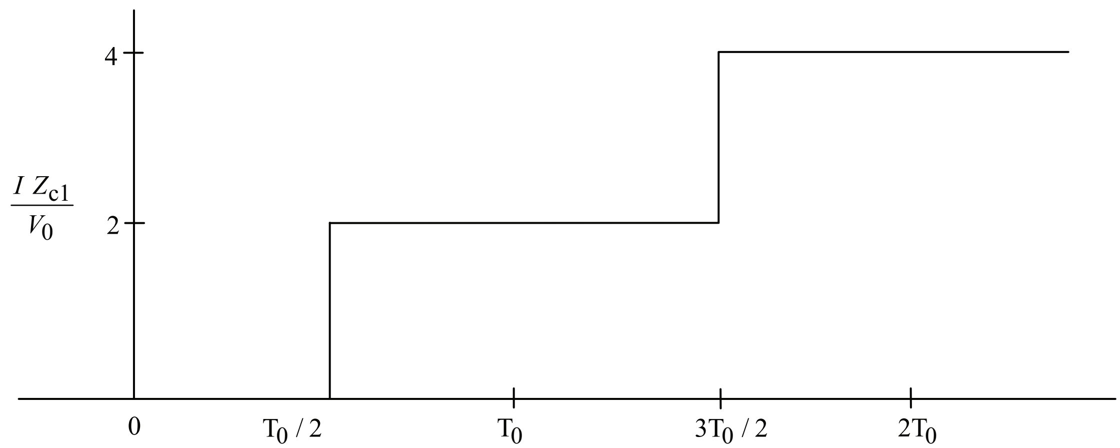

B. Current at far ends

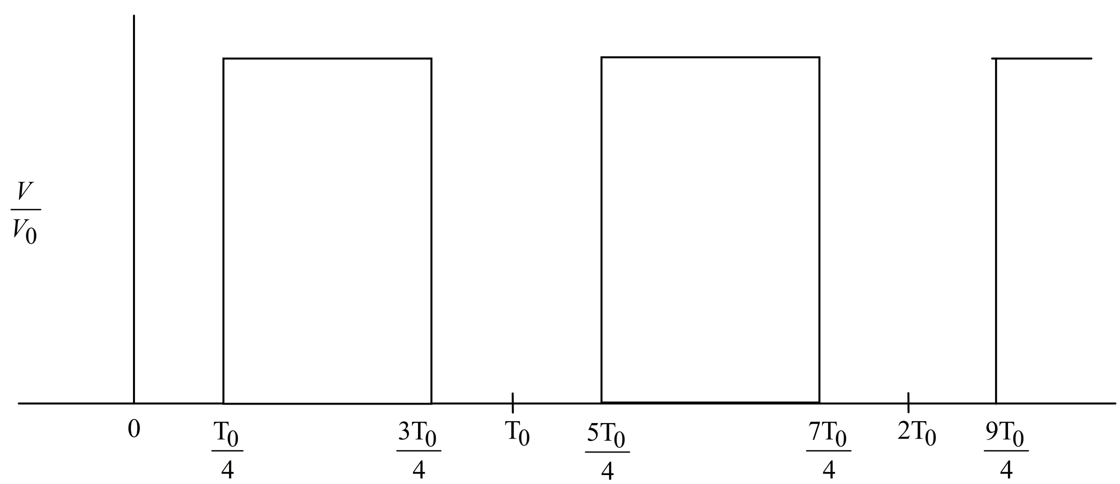

C. Voltage in middle of right section

Fig. 2.3 Ideal Waveforms

3. Extracting the Oscillatory Signal

3.1 End extraction by sampling current

Now consider some techniques for extracting the desired oscillatory signal. Figure 3.1 shows one such approach. The signal is extracted on a transmission line of characteristic impedance Z_{c2} with

$$Z_{c2} \ll Z_{c1} \tag{3.1}$$

Noting that the waveform in Fig. 2.3B has characteristic frequencies

$$f = f_1, f_2, f_3, \ldots, \quad f_n = nf_1 = \frac{n}{\mathrm{T}_0} \tag{3.2}$$

given by the harmonic series, it becomes a question of selecting the desired one (or more) to deliver to the antenna.

To better understand this type of excitation, note that the voltage delivered to the output is

$$\begin{aligned} V_1 &= [1 + \rho] V_0 \\ \rho &= \frac{Z_{c2} - Z_{c1}}{Z_{c2} + Z_{c1}} \\ 1 + \rho &= \frac{2Z2}{Z_{c2} + Z_{c1}} \simeq 2\frac{Z_{c2}}{Z_{c1}} \end{aligned} \tag{3.3}$$

For the first voltage step (at $T_0 / 2$), and subsequent steps at every additional T_0 .

To estimate the oscillation at frequency f_1, period T_0, first cut V_1 in half but repeat it with minus sign at T_0 (or $T_0 / 2$ after first step). Continuing (ad nauseum) gives a waveform like that in Fig. 2.3C. This looks like a square-wave oscillation with amplitude $4 / \pi$ corresponding to a sinusoidal oscillation of amplitude $\pm V_1 / 4$ times this [5], or

$$V_2 = \frac{V_1}{\pi} \simeq \frac{2}{\pi}\frac{Z_{c2}}{Z_{c1}} V_0 \tag{3.4}$$

s

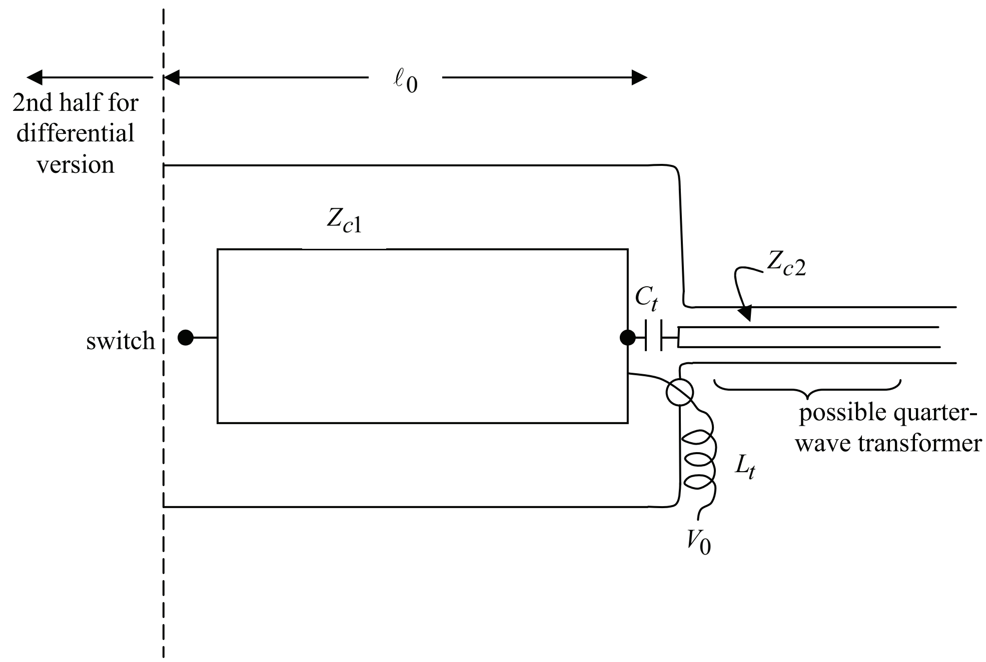

Figure 3.1 End Extraction

as the f_1 oscillation amplitude. This, of course, decays as a damped sinusoid as in a previous discussion [8]. Adapting this to the present case we have a geometric series with amplitude decaying as $[-\rho]^N$ (instead of $2N$) after N cycles. Setting this to e^{-1} we have

$$\begin{aligned} N &= -\ell n^{-1}(-\rho) = -\ell n^{-1}\left(1-2\frac{Z_{c2}}{Z_{c1}}\right) \\ &\simeq \frac{Z_{c2}}{2\,Z_{c1}} \\ Q &= \pi N \simeq \frac{\pi}{2}\frac{Z_{c1}}{Z_{c2}} \end{aligned} \tag{3.5}$$

Of course, there are various other losses for which this does not account.

With a small Z_{c2} one may wish to raise this to some larger value, say Z_{c3}, corresponding to some antenna impedance. In this case we may wish some intermediate impedance Z'_{c2} (quarter-wavelength long) as

$$Z'_{c2} = \left[Z_{c2}\,Z_{c3}\right]^{1/2} \tag{3.6}$$

with Z_{c2} now as still the input impedance at f_1. However, for $f \simeq f_1$ the situation is more complicated.

Note in Fig. 3.1 another possible design feature. We may have some impedance (indicated here as an inductance L_t) which allows low-frequency charging currents to flow through it, instead of the antenna. Of course this must also be a high impedance (compared to Z_{c2}) for frequencies near f_1.

Having understood the extraction procedure for f_1, one can go on to higher f_n. Their amplitudes are, of course, progressively smaller, and can be computed by a similar procedure to the foregoing, in which the V_1 step is further subdivided to correspond to each such frequency. Of course, one can obtain the same result by a Fourier integral.

3.2 Distributed center extraction of voltage

An alternate extraction procedure is illustrated in Fig. 3.2. In this case we have a second transmission-line conductor weakly coupled to the primary oscillator. To better understand this configuration, consider the open-circuit voltage at the connection to the second transmission-line conductor. Ideally we have on the main transmission line

$$\tilde{V}_{os}(z,s) = \frac{V_0}{s} \frac{e^{-\gamma z} - e^{-2\gamma\ell_0} e^{\gamma z}}{1 - e^{-2\gamma\ell_0}} \tag{3.6}$$

At the pickoff position ($z = \ell_0 / 2$) we have an open-circuit voltage on the second transmission-line conductor of

$$\tilde{V}_{oc}(s) = f_{out}\, \tilde{V}_{os}\left(\frac{\ell_0}{2}, s\right) = f_{out}\, e^{-\frac{\gamma\ell_0}{2}} \frac{1 - e^{-\gamma\ell_0}}{1 - e^{-2\gamma\ell_0}} \tag{3.7}$$

where f_{out} is a geometric factor representing the fraction of the oscillator voltage coupling to the second conductor with

$$0 = f_{out} \ll 1 \tag{3.8}$$

This is governed by how much the conductor is “exposed” to the main oscillator.

We still have at our disposal the length of this parasitic conductor with

$$0 < 2\ell_1 \leq \ell_0 \tag{3.9}$$

This length enters into the impedance V_{oc} drives as

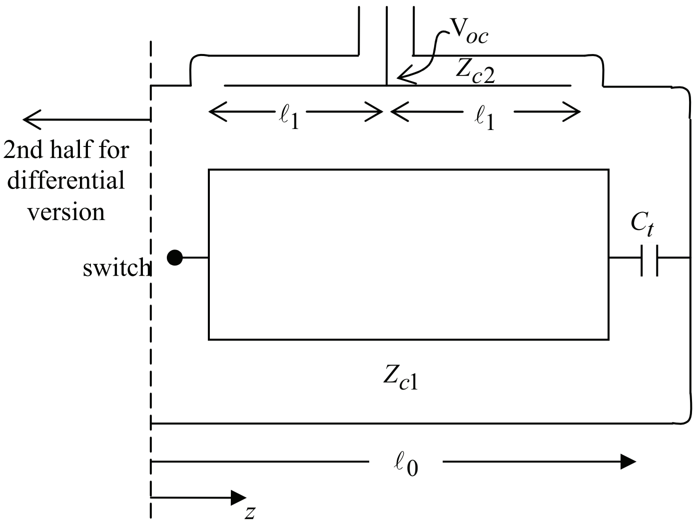

A. Side view

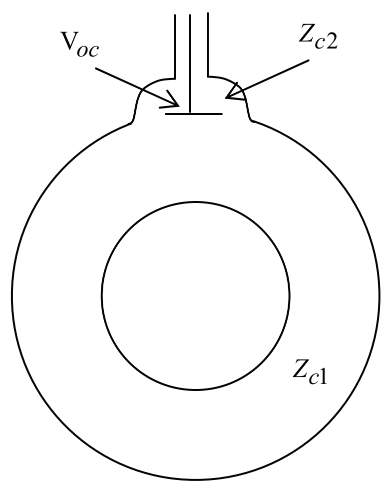

B. Cross section in center of right half

Figure 3.2 Second Transmission-Line Conductor Connected to Output: Center Extraction

$$\tilde{Z}_2(s) = Z_3 + Z_{c2} \frac{1+e^{-2\gamma\ell_1}}{1-e^{-2\gamma\ell_1}} \tag{3.10}$$

By adjusting ℓ_1 various response characteristics can be achieved. The length ℓ_1 itself can be considered a quarter-wave oscillator which may or may not be matched to the half wave oscillator by $2\ell_1 = \ell_0$.

As long as f_{out} is sufficiently small one can estimate the performance by calculating the power into $\tilde{Z}_2$ in one cycle, and comparing this to the energy in the main oscillation frequency (about 80% of the total stored energy [5]). This determines the Q (or N cycles to e^{-1}) as in [5, 8].

A fuller analysis would consider the propagation of waves as a 2 x 2 matrix on the two-conductor (plus reference) transmission line [6].

By adjusting ℓ_1 one can also vary the amount of higher harmonics in the output relative to the main oscillation. By moving the center of the output connection away from $z = \ell_0 / 2$ one can also reintroduce the second harmonic ($2f_1$) as well as change the relative coupling of the other harmonics to the output.

3.3. Triaxial Evolution

Between the switch and short circuit in region 1 is a half wavelength. However, the physical length can be made less by increasing ε_1, and/or making the reentrant geometry in Fig. 4.1. For simplicity, we consider the configuration on a plane containing the rotation axis. By varying the length of the inner coaxial region we can vary the outer length of the oscillator region as one desires.

The oscillator now has a triaxial structure (and can in principle go to higher order multiaxes). Including the inner coax leading to the load this is now a quadraxial structure. Of course, we could extend the innermost coaxial section back toward the switch, but this would reduce the overall length to about $\lambda_1 / 4$ (or $\ell_0 / 2$), a condition we may wish to avoid. In addition for a given outer oscillator radius we are more limited in the charge voltage, V_0, we can apply. So this technique may be more appropriate for low-frequency oscillators.

Here we can also have

$$Z_{c1}^{(1)} \neq Z_{c1}^{(2)} \tag{4.1}$$

if desired. This gives additional flexibility at the expense of analytic complexity. With equality, the previous analysis applies.

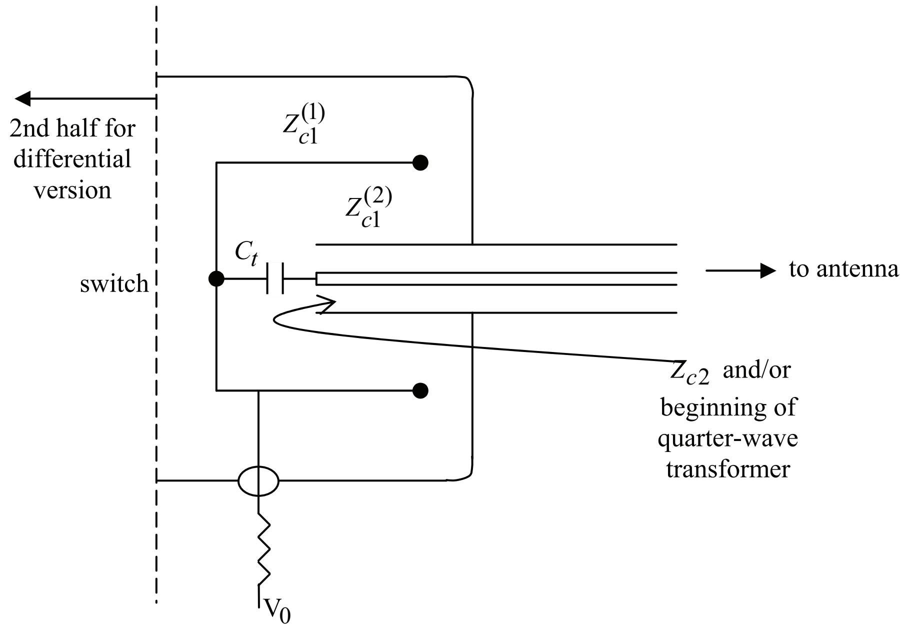

Fig. 4.1 Qusdraxial Oscillator Geometry.

3.4. Extraction of Third Harmonic

One of the problems with switched-oscillator design concerns the blocking capacitor which stores much energy, thereby loading the pulse-power system which charges the oscillator. Let us consider incorporating this capacitor into the switched-oscillator design. Let us make it an open-circuited quarter-wave transmission line tuned to the desired oscillator frequency

$$f_1 = \frac{c}{\lambda_1} = \frac{c}{2\ell_0} \tag{5.1}$$

with a physical length of $\ell_0 / 2$. Again we are sampling the current at a current maximum for this frequency.

Note, now, that the antenna is still *not charged* in a DC sense, before the switch fires. Furthermore, during the charging cycle, *much less charge* passes through the antenna (with potential held near zero).

Figure 5.1 shows some potential configurations for such a switched oscillator. This shows an extension of the center conductor beyond ℓ_0 to $3\ell_0 / 2$, the extension being the quarter-wave oscillator which looks like a short-circuit at f_1. The output to the antenna or transformer remains at (or near) ℓ_0, the output of the half-wave oscillator.

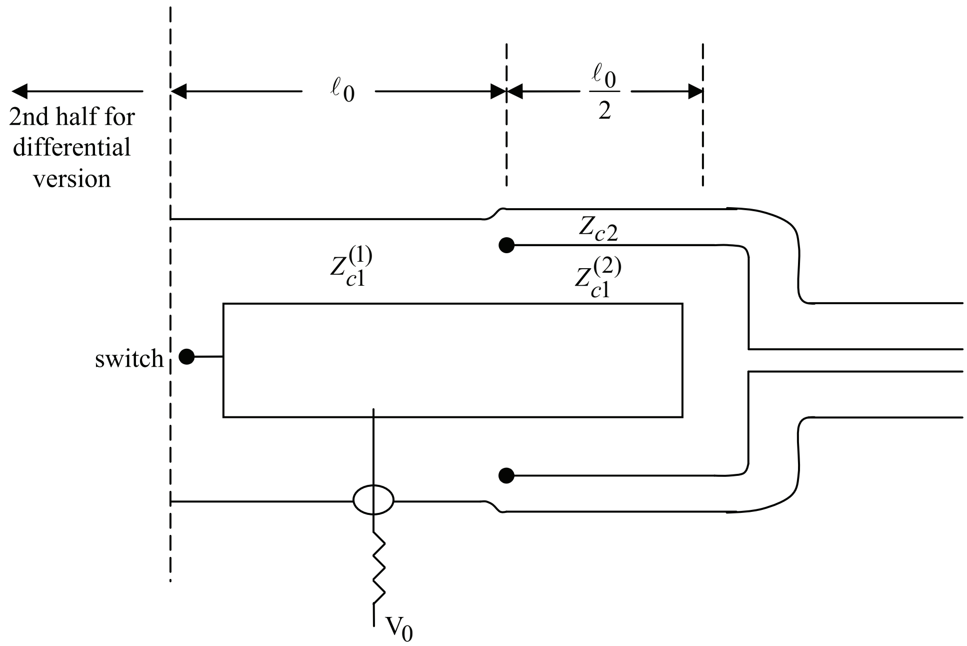

Fig. 5.1 Compound Switched Oscillator

But wait a minute! Suppose that

$$Z_{c1}^{(1)} = Z_{c1}^{(2)} \tag{5.2}$$

so that the line is uniform (except for the small perturbation into Z_{c2}). The entire conductor of length $3\ell_0 / 2$ is then a half-wave resonator with

$$\begin{aligned} \lambda_1' &= 3\ell_0 = 3\lambda_1 \\ f_1' &= \frac{c}{\lambda_1'} = \frac{1}{3} f_1 \end{aligned} \tag{5.3}$$

Beginning a new series of odd harmonics.

Of course, we do not need to have a uniform transmission-line oscillator. The now two sections can each have different values for Z_{c1}. For example, $Z_{c1}^{(2)}$ might be made smaller than the other to try to clamp the voltage at the input to this section. However, this is moving in the direction of C_t which we wanted to reduce. Perhaps this calls for some compromise.

6. Concluding Remarks

By using a more complex topology, one can increase the design options for switched oscillators. Such multiaxial structures also allow for greater oscillator length for a given frequency. This can be useful at high frequencies. These options are also appropriate for driving low impedances, instead of high impedances.

Note the basic limits on high-voltage switching speeds [7]. This indicates faster speeds when switching into higher impedances. Such is the case for some of the design options.

References

1. C. E. Baum, "A Technique for the Distribution of Signal Inputs to Loops", Sensor and Simulation Note 23, July 1966.

2. C. E. Baum, "Antennas for the Switched-Oscillator Source", Sensor and Simulation Note 455, March 2001.

3. C. E. Baum, "Differential Switched Oscillators and Associated Antennas", Sensor and Simulation Note 457, June 2001.

4. C. E. Baum, "Differential Switched Oscillators and Associated Antennas, Part 2", Sensor and Simulation Note 484, November 2003.

5. C. E. Baum, "Combined Electric and Magnetic Dipoles for Mesoband Radiation, Part 2", Sensor and Simulation Note 531, May 208.

6. C. E. Baum, T. K. Liu, and F. M. Tesche, "On the Analysis of General Multiconductor Transmission-Line Networks", Interaction Note 350, November 1978.

7. J. M. Lehr, C. E. Baum, and W. D. Prather, "Fundamental Physical Considerations for Ultrafast Spark Gap Switching", Switching Note 28, Nune 1997; also pp. 11-20 in E. Heyman et al (eds.), *Ultra-Wadeband, Short-Pulse Electromagnetics 4*, Kluwer Academic/Plenum Publishers, 1999.

8. 8. C. E. Baum, "Switched Oscillators", Circuit and Electromagnetic Circuit Design Note 45, September 2000.

9. C. E. Baum, "A Transmission-Line Transformer for Matching the Switched Oscillator to a Higher-Impedance Resistive Load", Circuit and Electromagnetic System Design Note 46, August. 2001.

10. C. E. Baum, "Some Thoughts Concerning Extending the Performance of Switched Oscillators", Circuit and Electromagnetic System Design Note 54, March 2008.

11. J. Burger et al, "Modular Low Frequency High Power Microwave Generator", AMEREM 2002, Annapolis, Maryland.

12. C. E. Baum and H. N. Kritokos, "Symmetry in Electromagnetics", ch. 1, pp. 1-90, in C. E. Baum and H. N. Kritikos (eds.), *Electromagnetic Symmetry*, Taylor & Francis, 1995.